


## Article

# The Effect of Grain Orientation of $\beta$ -Sn on Copper Pillar Solder Joints during Electromigration

Kexin Xu <sup>2,3,4</sup>, Xing Fu <sup>1,3,\*</sup> , Xinjie Wang <sup>2,4</sup>, Zhiwei Fu <sup>3</sup>, Xiaofeng Yang <sup>3</sup>, Si Chen <sup>3</sup>, Yijun Shi <sup>3</sup>, Yun Huang <sup>3</sup> and Hongtao Chen <sup>2,4,\*</sup>

- <sup>1</sup> School of Electronics and Information, South China University of Technology, Guangzhou 510640, China  
<sup>2</sup> Department of Materials Science and Engineering, Harbin Institute of Technology, Shenzhen 518055, China; 19s155065@stu.hit.edu.cn (K.X.); 19s155068@stu.hit.edu.cn (X.W.)  
<sup>3</sup> Department of Reliability Design Research, China Science and Technology on Reliability Physics and Application of Electronic Component Laboratory, Guangzhou 510610, China; fuzhiwei@ceprei.com (Z.F.); yxf004@hotmail.com (X.Y.); chensi@ceprei.com (S.C.); shiyijun@ceprei.com (Y.S.); huangyun@ceprei.com (Y.H.)  
<sup>4</sup> Sauvage Laboratory for Smart Materials, Harbin Institute of Technology (Shenzhen), Shenzhen 518055, China  
\* Correspondence: fuxing@ceprei.com (X.F.); chenht@hit.edu.cn (H.C.)

**Abstract:** The grain orientation of Sn-based solder joints on copper pillars under the combined action of electron wind force and temperature gradient greatly affects their electromigration damage. The copper pillars with Sn-1.8Ag lead-free solder on the top was subjected to a current density of  $1.5 \times 10^4$  A/cm<sup>2</sup> at 125 °C to study the electromigration behaviors. The grain orientation was characterized by scanning electron microscopy (SEM) equipped with electron backscattered diffraction (EBSD) detector. Metal dissolution and voids formation in the cathode as well as massive intermetallic compounds (IMC) accumulation in the anode were observed after electromigration. Closer examination of solder joints revealed that the Sn grain whose c-axis perpendicular to electric current may have retarded Cu diffusion to anode and IMC accumulation. In addition, the newly formed Cu<sub>6</sub>Sn<sub>5</sub> exhibited preferred orientation related to the electric current direction.

**Keywords:** copper pillar; electromigration; grain orientation; IMC accumulation; preferred orientation



**Citation:** Xu, K.; Fu, X.; Wang, X.; Fu, Z.; Yang, X.; Chen, S.; Shi, Y.; Huang, Y.; Chen, H. The Effect of Grain Orientation of  $\beta$ -Sn on Copper Pillar Solder Joints during Electromigration. *Materials* **2022**, *15*, 108. <https://doi.org/10.3390/ma15010108>

Academic Editor: Antonio Riveiro

Received: 20 October 2021

Accepted: 12 December 2021

Published: 24 December 2021

**Publisher's Note:** MDPI stays neutral with regard to jurisdictional claims in published maps and institutional affiliations.



**Copyright:** © 2021 by the authors. Licensee MDPI, Basel, Switzerland. This article is an open access article distributed under the terms and conditions of the Creative Commons Attribution (CC BY) license (<https://creativecommons.org/licenses/by/4.0/>).

## 1. Introduction

As the miniaturization and high-performance requirement of microelectronic devices continue to increase, micro-bumps become the mainstream trend in high-density packaging [1,2]. Copper pillar solder joints exhibited excellent properties in electrical conductivity and thermal conductivity, and have been used as the main interconnection method in the case of below 100  $\mu$ m fine pitch [3–7]. However, the volume of solder used for bonding would shrink significantly, with the transition from C4 joints (controlled collapse chip connection) to copper pillar joints. Many reliability issues emerge owing to the shrinking solder volume [8,9]. One such issue is that the increasing current density through each copper pillar may exceed the electromigration threshold ( $10^4$  A/cm<sup>2</sup>), which causes the electromigration damage [10].

Most of the lead-free solders used at present are tin-rich, which usually contain more than 90% Sn, indicating that the properties of lead-free solders are dictated by the properties of pure Sn [11–14]. Due to the downsizing of solder used in copper pillar, there are only limited  $\beta$ -Sn grains.  $\beta$ -Sn has a lattice structure of body-centered tetragonal ( $a = b = 5.83$  Å,  $c = 3.18$  Å), whose physical, chemical properties are highly anisotropic [14–16]. When solder joints contain single or several grains, the anisotropy of  $\beta$ -Sn will severely affect the integrity and reliability of lead-free solder joints.

The detailed report of Lu et al. [17] indicated the formation of IMC along grain boundary parallel to the current flow in bi-crystal Sn grain solder joints containing two grains with very different orientations. If the c axis of the grain is more parallel to the current flow,

IMC will grow rapidly due to the rapid diffusion of Cu. If the *c* axis of the grain is more perpendicular to the current flow, IMC accumulation would be suppressed due to the retardation of Cu towards anode. Shen [18] reported that the sample with  $\alpha$  angle lower than  $25^\circ$  ( $\alpha$  was defined as the angle between *c* axis of Sn grain and current flow) exhibited fast accumulation of interfacial IMC by drawing a relationship between the average  $\alpha$  in the solder joints with the thickness of the interfacial IMC in electromigration experiments on a few solder joints composed of several grains with different  $\alpha$ . Huang [19] noticed that when electrons flowed from the  $\beta$ -Sn grains with smaller  $\alpha$  to the adjacent grains with high  $\alpha$ , a large amount of IMC was accumulated at the grain boundary, because the migration of Cu atoms from the grain boundary to the anode was hindered, and a large amount of columnar  $\text{Cu}_6\text{Sn}_5$  IMCs was precipitated in the  $\beta$ -Sn grains with smaller  $\alpha$ . When electrons flowed from the grain with high  $\alpha$  to the grain with smaller  $\alpha$ , voids at the interface of Cu-solder formed and little IMC grew. Tian et al. [20] found that IMC growth can be seen when the *c* axis of the Sn grains was aligned with the electron flow direction towards the cross-sectional surface, as they could form a convex bulge on the surface of the sample. Additionally, the IMC growth behavior of one grain was not affected by the other grains in the single solder joint.

Although copper pillars are a popular interconnection method in 3-D packaging, there are few studies on the electromigration damage in this kind of solder joint. However, due to the limited solder volume and anisotropic property of each interconnect joint, chemical reactions may convert all solder to brittle intermetallic compounds. In this study, electromigration tests were conducted with the sample of Cu/Sn-1.8Ag/Cu microbumps under current density of  $1.5 \times 10^4 \text{ A/cm}^2$  at  $125^\circ\text{C}$ . SEM and EBSD images were utilized to reveal the relationship between electromigration damage and tin grain orientation.

## 2. Experiment

Figure 1a showed the dimension and structure of the copper pillar samples. The solder cap was electroplated on the copper pillar, and then the solder joint was reflowed to form a complete joint, which was shown in Figure 1a. The solder for bonding was Sn-1.8Ag solder with height of  $23.10 \mu\text{m}$  before joining. A small amount of IMC was formed at the interface between Cu substrate and solder during the bump fabrication. The diameter of copper pillar was  $46.10 \mu\text{m}$ , which was same as the diameter of solder mask. On the substrate of BT material side, the copper trace was  $7.2 \mu\text{m}$  thick. The pitch between two adjacent pillars was  $34.29 \mu\text{m}$ .

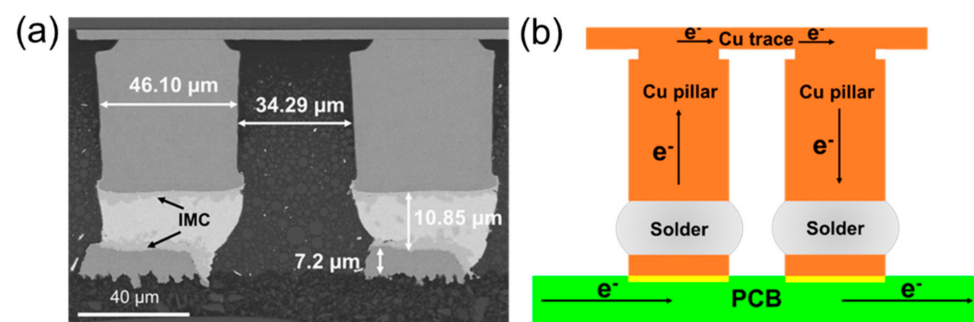


**Figure 1.** The structure of tested copper pillar joint: (a) The dimension and structure of the test samples after reflow; (b) the schematic diagram of experiment setup.

The applied current density loaded on copper pillar was  $1.5 \times 10^4 \text{ A/cm}^2$  at  $125^\circ\text{C}$ , the schematic diagram of experiment setup was shown in Figure 1b. After grinding and polishing, SEM and EBSD were conducted to examine microstructure evolution and the grain orientation, respectively. For easy understanding of Sn grain orientation,  $\alpha$  was defined as the angle between the *c*-axis of  $\beta$ -Sn and electron flow, describing the orientation of Sn grain in this study.

### 3. Results

#### 3.1. Microstructure Evolution of Cu Pillar after Electromigration Test

During the electromigration, atoms at the cathode diffused to the anode, forced by electron wind under the action of electrothermal coupling. As shown in Figure 2, the Ni layer and the Cu layer at the cathode were dissolved to different extent, dominated by the Ni and Cu flux induced by the current after current stressing at  $1.5 \times 10^4$  A/cm<sup>2</sup> at 125 °C for 200 h. Ni and Cu are interstitially diffused in the Sn matrix due to their low solubility in Sn [21,22]. The anode received a great number of Cu atoms from the cathode and a great amount of IMC accumulated, which mainly consisted of Cu<sub>6</sub>Sn<sub>5</sub> and Cu<sub>3</sub>Sn. Cu<sub>6</sub>Sn<sub>5</sub> and Cu<sub>3</sub>Sn were both the phases with high hardness and low strength, which could be the potential site for crack initiation. Under the action of stress, crack initiation and propagation may occur in the IMC layer. The fracture mode of solder joint may change from plastic mode to plastic-brittle mixed mode. The accumulation of Cu<sub>6</sub>Sn<sub>5</sub> and Cu<sub>3</sub>Sn had great influence on the reliability of copper pillar joints.

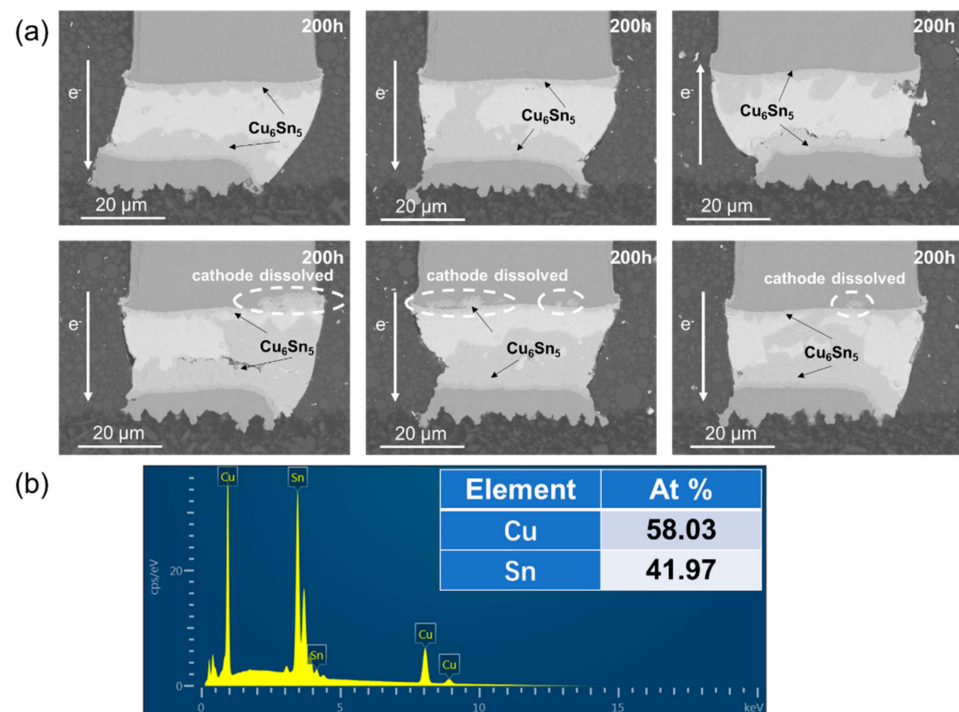


**Figure 2.** Microstructure after current stressing at  $1.5 \times 10^4$  A/cm<sup>2</sup> at 125 °C for 200 h: (a) SEM images of copper pillar joints (b) the EDS results of IMCs.

#### 3.2. The Effect of Grain Orientation on Electromigration Damage

The inherent intrinsic properties of  $\beta$ -Sn were key factors to the interstitial diffusion of Ni, Cu. The diffusion coefficients of Cu and Ni in the c axis could be 43 times and  $3 \times 10^4$  times than that in other directions at 150 °C, respectively [21,23]. Thus, characterization of grain structure was necessary for study on electromigration.  $\alpha$  was defined as the angle between c axis of Sn grain and electric current. As shown in Figure 3c, only two grains with different orientations were observed in the tested Sn matrix. The angle  $\alpha$  of the right blue  $\beta$ -Sn grain was 21.8°, massive Cu<sub>6</sub>Sn<sub>5</sub> IMC almost occupied the whole grain after 200 h electromigration test. In addition, the Cu pillar was partly dissolved in the right corner. The angle  $\alpha$  of the green  $\beta$ -Sn grain was 78.4° and the dissolution of the cathode Cu pillar was greatly retarded. Characterization for other interconnects under same test condition indicates that the two solder joints were comprised of grains with large  $\alpha$ , shown as Figure 4b,d. The angle  $\alpha$  of the yellow  $\beta$ -Sn grain was 86.3°, which mean the c axis of this grain was almost perpendicular to the electron flow direction. For the other solder joint, three differently oriented grains were all with large  $\alpha$  (70°, 89.7°, 72.2°). Due to the

lower diffusivity of Sn with orientation of large  $\alpha$ , the dissolution of the cathode Cu was limited and fewer IMC accumulated at the anode.

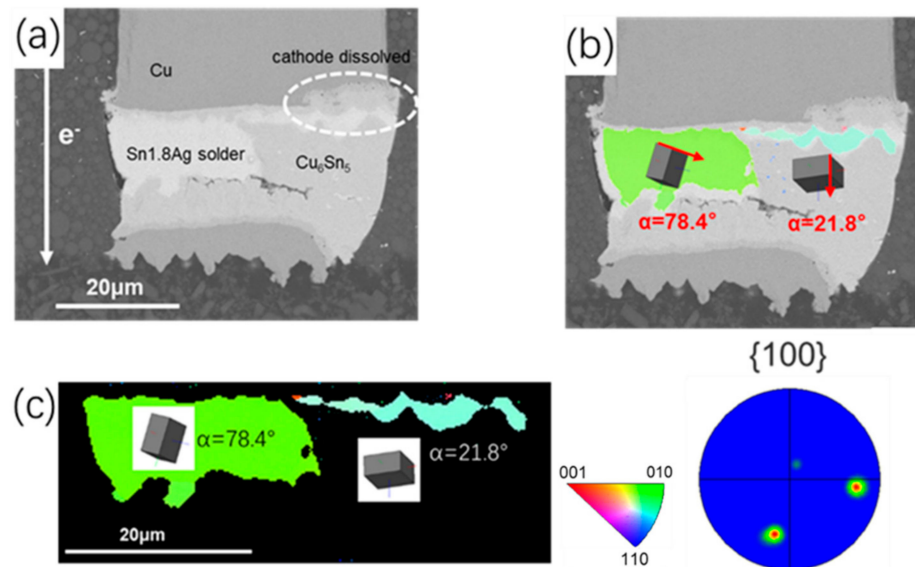


**Figure 3.** Microstructure after current stressing at  $1.5 \times 10^4$  A/cm<sup>2</sup> at 125 °C for 200 h: (a) SEM image for the bump with downward electron flow; (b) SEM image for the bump with downward electron flow with unit cells; (c) the EBSD image corresponding to (a).

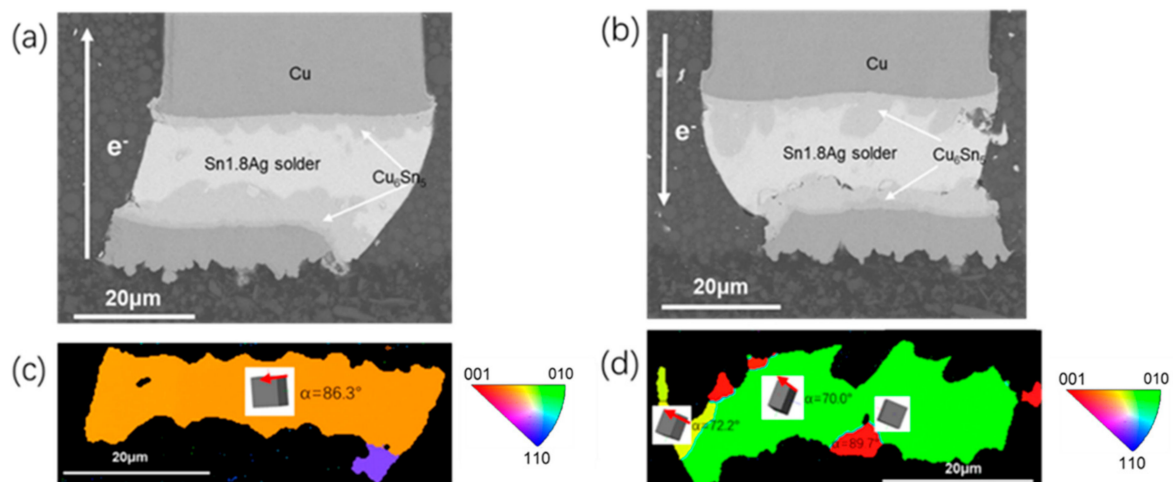


**Figure 4.** Microstructure after current stressing at  $1.5 \times 10^4$  A/cm<sup>2</sup> at 125 °C for 200 h: (a) SEM image for the copper pillar with upward current flow; (b) SEM image for the copper pillar with downward current flow; (c) the EBSD image corresponding to (a); (d) the EBSD image corresponding to (b).

To explore further into the effect of Sn orientation on the migration rate of Cu, the current stressing was terminated till 400 h. The tested sample was electrically stressed under  $1 \times 10^4$  A/cm<sup>2</sup> at 150 °C for 400 h. It turned out to that most of solder joints had changed to be full of IMC. From the SEM images of the copper pillar joints in Figure 5, it can be found the solder joints have taken on the structure of Cu/Cu<sub>3</sub>Sn/Cu<sub>6</sub>Sn<sub>5</sub>/Cu<sub>3</sub>Sn/Cu regardless of the current direction in the solder joints. However, under the same condition, many solder joints were still composed of Cu<sub>3</sub>Sn/Cu<sub>6</sub>Sn<sub>5</sub>/Sn/Cu<sub>6</sub>Sn<sub>5</sub>/Cu<sub>3</sub>Sn/Cu. As shown in Figure 6, in the unconsumed Sn, c axis of Sn grain was almost perpendicular to the electron flow. It can be seen in the solder joint with the grain orientation of large  $\alpha$ , there were many Sn matrix remained due to their stronger electromigration resistance. It was speculated that the reason for the solder joint full of IMC was that c axis of the Sn grain was closer to the current flow. In the cathode, some voids formed, which were caused by

the accumulation of vacancies. The copper and Sn atoms were gradually diffused to the anode by the electric current stressing, and in turn, the diffusion of the atoms resulted in a reverse vacancy flux. This flux of vacancies accumulated and formed voids eventually at the cathode.

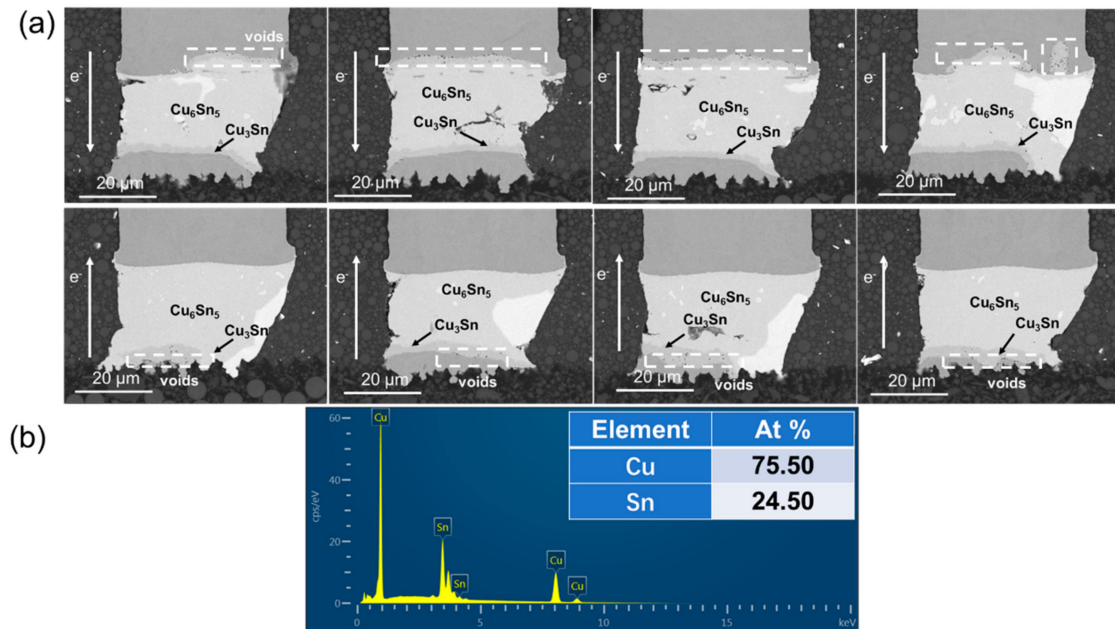


**Figure 5.** Microstructures of copper pillars full of IMCs after current stressing at  $1.5 \times 10^4$  A/cm<sup>2</sup> at 125 °C: (a) SEM images of copper pillar joints (b) the EDS results of IMCs.

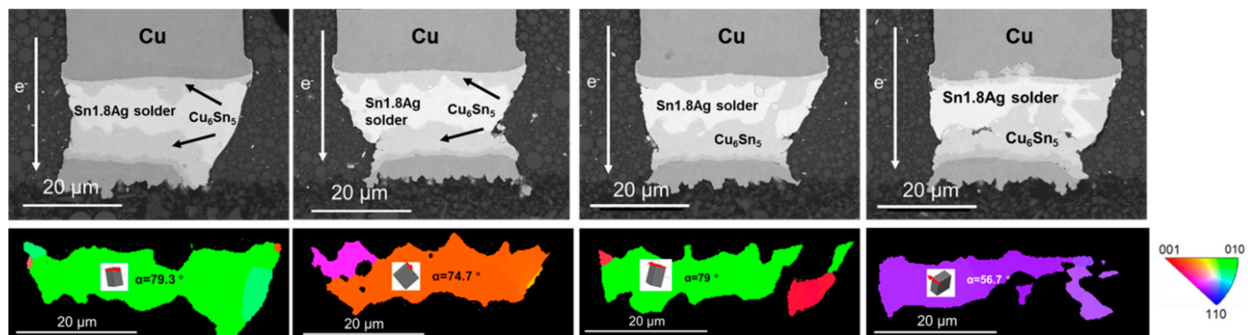


**Figure 6.** Microstructures of copper pillars with remained Sn after current stressing at  $1.5 \times 10^4$  A/cm<sup>2</sup> at 125 °C.

### 3.3. The Grain Structure of $\text{Cu}_6\text{Sn}_5$ during Electromigration

The grain structure of  $\text{Cu}_6\text{Sn}_5$  is critical for long-term service because the solder joints were likely to become full of IMC after a long period of operation. Microstructure morphology and grain structure of solder joints tested by electromigration for 600 h under  $1 \times 10^4$  A/cm<sup>2</sup> at 150 °C was shown in Figure 7. Several Sn grains whose orientations were unfavorable to the diffusion of copper atoms still existed, but most part of the solder joint had changed into IMC. A small amount of  $\text{Cu}_3\text{Sn}$  was found at the anode and most of IMC was  $\text{Cu}_6\text{Sn}_5$ , which was characterized to show hexagonal grain structure. Additionally, according to EBSD analysis, the newly formed  $\text{Cu}_6\text{Sn}_5$  exhibited preferred orientation related to the current direction. The (0001) plane of  $\text{Cu}_6\text{Sn}_5$ , the base of hexagonal grain structure, was considered to be the main plane through which electrons pass [21]. The carrier mobility was the main factor that affects the conductivity because the carrier concentration in a specific metal was close to a constant. In fact, the carrier mobility was inversely proportional to the resistivity, which depended mainly on the scattering of electrons by

the lattice. When electrons passed through a crystal plane with the lowest atomic density, they have the least lattice scattering, thus the direction perpendicular to that plane was the lowest resistance path. Therefore, the Sn grain whose (0001) crystal plane perpendicular to the current carries the lowest lattice scattering intensity and the largest diffusion flux of Cu atoms. The grains with lower resistivity would have greater current stress and hence higher atomic flux, so would grow preferentially by swallowing the grains with large resistivity. Therefore, this may be the reason for the preferential orientation of  $\eta$ -Cu<sub>6</sub>Sn<sub>5</sub> under current stress. However, the grain orientation of Cu<sub>6</sub>Sn<sub>5</sub> closer to the substrate was rather disordered, which was probably owing to the preferred orientation of Cu<sub>6</sub>Sn<sub>5</sub> and copper substrate during solder joint reflow. As electric current stressing continued to load, large grains of Cu<sub>6</sub>Sn<sub>5</sub> grew by swallowing the small ones, finally leading to the disappearance of fine grains. During aging, the newly formed Cu<sub>6</sub>Sn<sub>5</sub> in the middle exhibited preferred orientation related to the current direction more obviously. Thus, it can be concluded that the grain boundaries of Cu<sub>6</sub>Sn<sub>5</sub> moved by merging the fine grains with the random orientations.

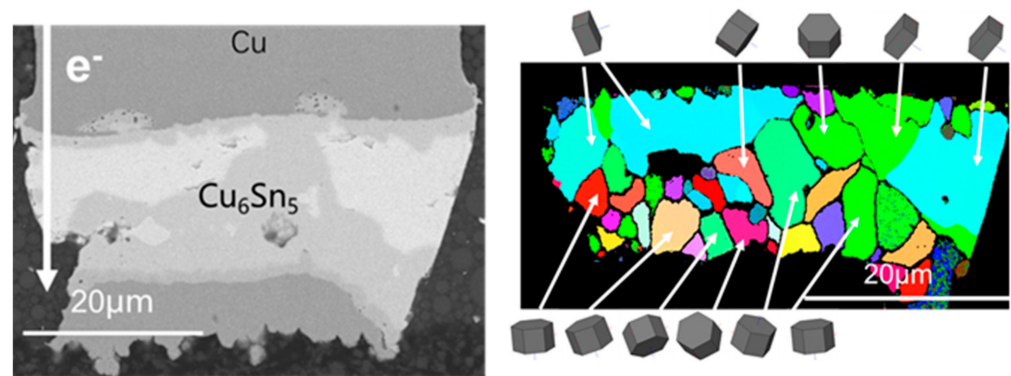


**Figure 7.** Microstructure after current stressing at  $1.5 \times 10^4$  A/cm<sup>2</sup> at 125 °C for 600 h.

### 3.4. Microhardness and Elastic Modulus of IMCs in Copper Pillar Joint after Electromigration Test

Microstructure morphology, nanoindentation on Cu<sub>6</sub>Sn<sub>5</sub> and Cu<sub>3</sub>Sn and grain structure of solder joint tested by electromigration for 800 h under  $1 \times 10^4$  A/cm<sup>2</sup> at 150 °C was shown in Figure 8. The curve describing relationship between the value of load and indentation depth applied in nanoindentation experiment was shown in Figure 9. Sixteen different positions on Cu<sub>6</sub>Sn<sub>5</sub> from four different solder joints was selected for indentation experiments to obtain Young's modulus and microhardness of Cu<sub>6</sub>Sn<sub>5</sub>. According to the Oliver–Pharr method, the hardness,  $H$ , was expressed as [24]

$$H = \frac{P_{max}}{A(h_c)}$$

where  $A(h_c)$  was the contact area and  $P_{max}$  was the maximum load. To obtain the Young's modulus  $E$ ,  $E_r$  was indispensable to know, defined as the reduced Young's modulus by elastic recovery of the sample and the indentation, which can be calculated by [24]

$$E_r = \frac{\sqrt{\pi}}{2\beta} \frac{S}{\sqrt{A}}$$

where  $\beta$  was a constant relevant to the indentation,  $S$  was the slope of the top point of the unloading curves of Load–Depth, and  $A$  was the project contact area. Thus, the Young's modulus  $E$  can be obtained by [24,25]

$$E_r = \left( \frac{E}{1 - \nu^2} + \frac{E_I}{1 - \nu_I^2} \right)^{-1}$$

where the  $\nu$  and  $\nu_I$  were Poisson's ratio of sample and the indentation.  $E_I$  was the Young's modulus of the indentation. The results showed the average values of Young's modulus and microhardness of  $\text{Cu}_6\text{Sn}_5$  were  $118.24 \pm 6.42$  GPa and  $6.72 \pm 0.54$  GPa, respectively. The same experiment was also conducted on  $\text{Cu}_3\text{Sn}$ . Ten different positions on  $\text{Cu}_3\text{Sn}$  from four different solder joints was selected for indentation experiments to measure Young's modulus and microhardness of  $\text{Cu}_3\text{Sn}$ . The results showed the average values of Young's modulus and microhardness of  $\text{Cu}_6\text{Sn}_5$  were determined to be  $147.67 \pm 6.42$  GPa and  $6.46 \pm 0.54$  GPa, respectively. According to the reports of Deng et al. [26] the Young's modulus and microhardness of Cu of the pillar was  $116.50 \pm 4.70$  GPa and  $1.65 \pm 0.17$  GPa. The result of nanoindentation experiment revealed that there is Young's modulus mismatch between  $\text{Cu}_6\text{Sn}_5$ ,  $\text{Cu}_3\text{Sn}$  and Cu, which provided additional degradation mechanism.

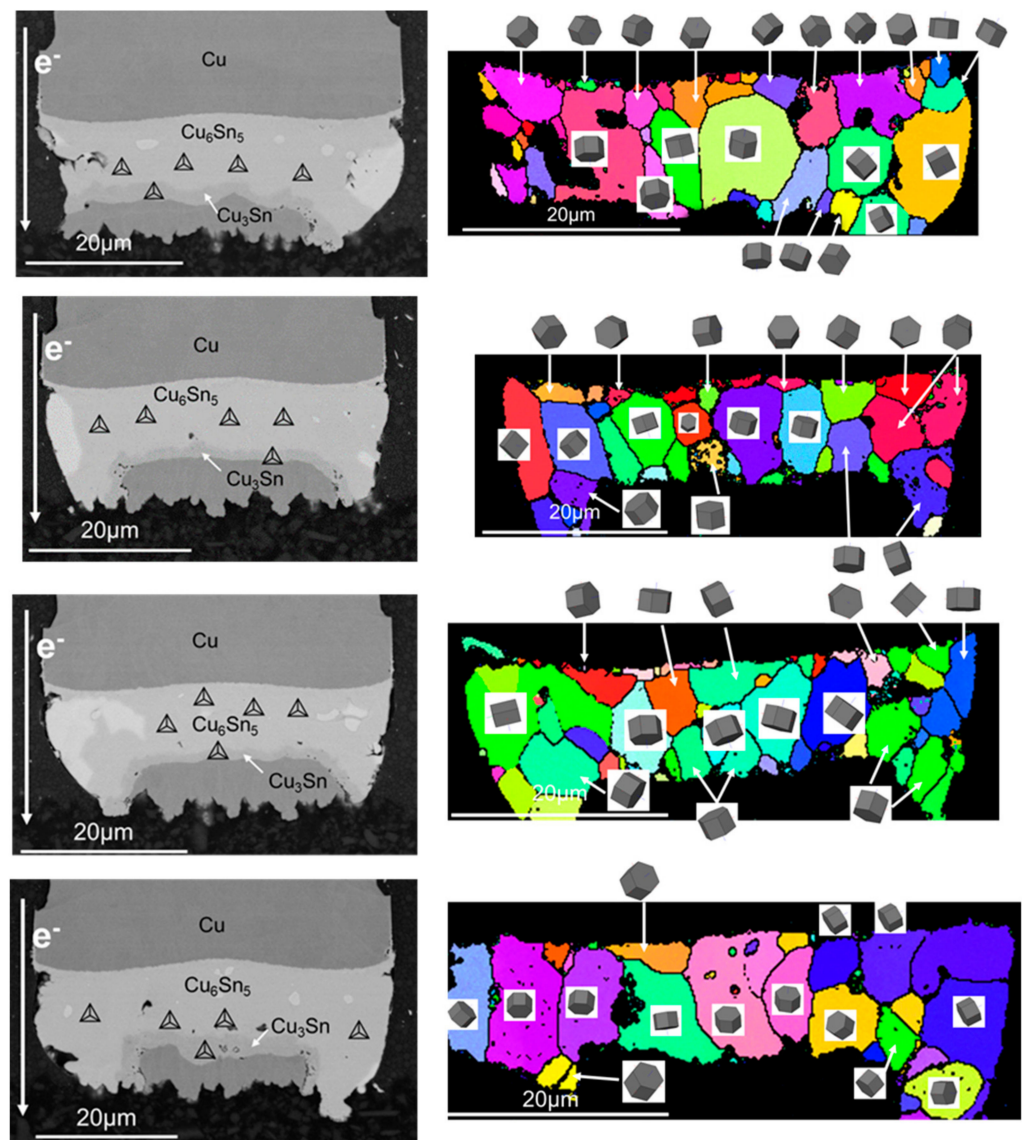


**Figure 8.** Microstructure after current stressing at  $1.5 \times 10^4$  A/cm<sup>2</sup> at 125 °C for 800 h.

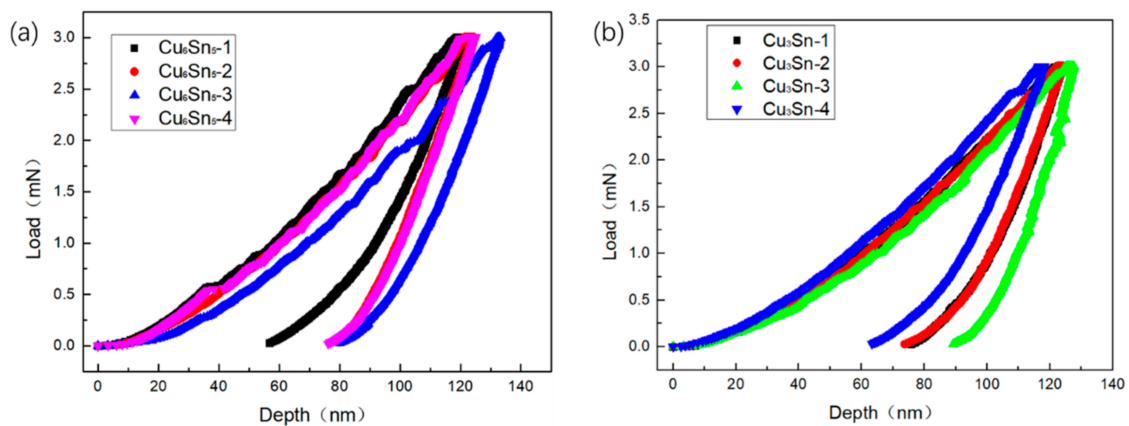


Figure 9. Curves of load vs indentation depth in nanoindentation experiment:(a) Cu<sub>6</sub>Sn<sub>5</sub>; (b) Cu<sub>3</sub>Sn.

#### 4. Conclusions

The microstructure and grain evolution of copper pillar solder joints after current stressing at  $1.5 \times 10^4$  A/cm<sup>2</sup> at 125 °C was studied by SEM and EBSD. During the electromigration, the anode received a large number of Cu atoms from the cathode and a large amount of IMC accumulated, which mainly consisted of Cu<sub>6</sub>Sn<sub>5</sub> and Cu<sub>3</sub>Sn. Kirkendall voids at the cathode formed due to the vacancies flux. The orientation of Sn grain had a considerable effect on diffusion of Cu and electromigration damage. The Sn grain with the large  $\alpha$  effectively retarded the Cu diffusion and IMC accumulation, exhibiting excellent electromigration resistance performance. EBSD analysis showed that the preferred orientation of hexagonal Cu<sub>6</sub>Sn<sub>5</sub> after electromigration was (1000). The nanoindentation experiment results of newly formed IMC, Cu<sub>6</sub>Sn<sub>5</sub> and Cu<sub>3</sub>Sn, revealed Young's modulus mismatch existed between Cu<sub>6</sub>Sn<sub>5</sub>, Cu<sub>3</sub>Sn and Cu, which provided additional degradation mechanism. This study provided better understanding of the microstructure/grain structure change and its effect on IMC formation in solder joint during electromigration.

**Author Contributions:** Investigation, X.F., S.C., X.Y., Y.S., Z.F., Y.H., X.W. and H.C. Writing—original draft, K.X.; Writing—review and editing, X.F., H.C. All authors have read and agreed to the published version of the manuscript.

**Funding:** This work is financially supported by Natural Science Foundation of China Youth Foundation (No.62004046), the foundation of Science and Technology on Reliability Physics and Application Technology of Electronic Component Laboratory (No. 61428060102-1and No.61428060201), the Natural Science Foundation of Guangdong Province (No. 2019A1515011844), and the Opening Project of Science and Technology on Reliability Physics and Application Technology of Electronic Component Laboratory (ZHD201801 and 31512050201).

**Conflicts of Interest:** The authors declare no conflict of interest.

#### References

1. Chaware, R.; Nagarajan, K.; Ramalingam, S. Assembly and Reliability Challenges in 3D Integration of 28 nm FPGA Die on a Large High Density 65 nm Passive Interposer. In Proceedings of the 2012 IEEE 62nd Electronic Components and Technology Conference, San Diego, CA, USA, 29 May–1 June 2012; pp. 279–283.
2. Charbonnier, J.; Assous, M.; Bally, J.-P.; Miyairi, K.; Sunohara, M.; Cuchet, R.; Hida, R. High density 3D silicon interposer technology development and electrical characterization for high end applications. In Proceedings of the 2012 4th Electronic System-Integration Technology Conference, Amsterdam, The Netherlands, 17–20 September 2012; pp. 1–7.
3. Kim, M.-S.; Kang, M.-S.; Bang, J.-H.; Lee, C.-W.; Kim, M.-S.; Yoo, S. Interfacial reactions of fine-pitch Cu/Sn–3.5Ag pillar joints on Cu/Zn and Cu/Ni under bump metallurgies. *J. Alloys Compd.* **2014**, *616*, 394–400. [[CrossRef](#)]
4. Bao, A.; Zhao, L.; Sun, Y.; Han, M.; Yeap, G.; Bezuk, S.; Lee, K. Challenges and opportunities of chip package interaction with fine pitch Cu pillar for 28 nm. In Proceedings of the 2014 IEEE 64th Electronic Components and Technology Conference (ECTC), Orlando, FL, USA, 27–30 May 2014; pp. 47–49.
5. Tu, K.-N.; Hsiao, H.Y.; Chen, C. Transition from flip chip solder joint to 3D IC microbump: Its effect on microstructure anisotropy. *Microelectron. Reliab.* **2013**, *53*, 2–6. [[CrossRef](#)]



6. Hsu, H.H.; Huang, Y.T.; Huang, S.Y.; Chang, T.C.; Wu, A.T. Evolution of the Intermetallic Compounds in Ni/Sn-2.5Ag/Ni Microbumps for Three-Dimensional Integrated Circuits. *J. Electron. Mater.* **2015**, *44*, 3888–3895. [[CrossRef](#)]
7. Liu, Y.; Chu, Y.C.; Tu, K.-N. Scaling effect of interfacial reaction on intermetallic compound formation in Sn/Cu pillar down to 1  $\mu\text{m}$  diameter. *Acta Mater.* **2016**, *117*, 146–152. [[CrossRef](#)]
8. Lee, K.; Kim, K.-S.; Tsukada, Y.; Suganuma, K.; Yamanaka, K.; Kuritani, S.; Ueshima, M. Influence of crystallographic orientation of Sn–Ag–Cu on electromigration in flip-chip joint. *Microelectron. Reliab.* **2011**, *51*, 2290–2297. [[CrossRef](#)]
9. Li, X.P.; Xia, J.M.; Zhou, M.B.; Ma, X.; Zhang, X.P. Solder Volume Effects on the Microstructure Evolution and Shear Fracture Behavior of Ball Grid Array Structure Sn-3.0Ag-0.5Cu Solder Interconnects. *J. Electron. Mater.* **2011**, *40*, 2425–2435. [[CrossRef](#)]
10. Jung, Y.; Yu, J. Electromigration induced Kirkendall void growth in Sn-3.5Ag/Cu solder joints. *J. Appl. Phys.* **2014**, *115*, 83708. [[CrossRef](#)]
11. Huang, M.L.; Zhao, J.F.; Zhang, Z.J.; Zhao, N. Role of diffusion anisotropy in  $\beta$ -Sn in microstructural evolution of Sn-3.0Ag-0.5Cu flip chip bumps undergoing electromigration. *Acta Mater.* **2015**, *100*, 98–106. [[CrossRef](#)]
12. Suh, D.; Kim, D.W.; Liu, P. Effects of Ag content on fracture resistance of Sn–Ag–Cu lead-free solders under high-strain rate conditions. *Mater. Sci. Eng. A* **2007**, *460*, 595–603. [[CrossRef](#)]
13. Anderson, I.E.; Foley, J.C.; Cook, B.A. Alloying effects in near-eutectic Sn-Ag-Cu solder alloys for improved microstructural stability. *J. Electron. Mater.* **2001**, *30*, 1050–1059. [[CrossRef](#)]
14. Kim, K.S.; Huh, S.H.; Suganuma, K. Effects of fourth alloying additive on microstructures and tensile properties of Sn–Ag–Cu alloy and joints with Cu. *Microelectron. Reliab.* **2003**, *43*, 259–267. [[CrossRef](#)]
15. Chen, H.; Hang, C.; Fu, X.; Li, M. Microstructure and Grain Orientation Evolution in Sn-3.0Ag-0.5Cu Solder Interconnects Under Electrical Current Stressing. *J. Electron. Mater.* **2015**, *44*, 3880–3887. [[CrossRef](#)]
16. Fu, X.; Liu, M.; Xu, K.; Chen, S.; Shi, Y.; Fu, Z.; Yao, R. The In-Situ Observation of Grain Rotation and Microstructure Evolution Induced by Electromigration in Sn-3.0Ag-0.5Cu Solder Joints. *Materials* **2020**, *13*, 5497. [[CrossRef](#)] [[PubMed](#)]
17. Lu, M.; Shih, D.-Y.; Lauro, P.; Goldsmith, C.; Henderson, D.W. Effect of Sn grain orientation on electromigration degradation mechanism in high Sn-based Pb-free solders. *Appl. Phys. Lett.* **2008**, *92*, 211909. [[CrossRef](#)]
18. Shen, Y.A.; Chen, C. Effect of Sn grain orientation on formation of Cu<sub>6</sub>Sn<sub>5</sub> intermetallic compounds during electromigration. *Scr. Mater.* **2017**, *128*, 6–9. [[CrossRef](#)]
19. Huang, M.L.; Zhao, J.F.; Zhang, Z.J.; Zhao, N. Dominant effect of high anisotropy in  $\beta$ -Sn grain on electromigration-induced failure mechanism in Sn-3.0Ag-0.5Cu interconnect. *J. Alloys Compd.* **2016**, *678*, 370–374. [[CrossRef](#)]
20. Han, J.; Guo, F. Nucleation and electromigration-induced grain rotation in an SABI333 solder joint. *J. Mater. Sci.* **2018**, *53*, 6230–6238. [[CrossRef](#)]
21. Dyson, B.F.; Anthony, T.R.; Turnbull, D. Interstitial Diffusion of Copper in Tin. *J. Appl. Phys.* **1967**, *38*, 3408. [[CrossRef](#)]
22. Tu, K.-N. Interdiffusion and Reaction in Bimetallic Cu-Sn Thin Films. *Acta Metall.* **1973**, *21*, 347–354. [[CrossRef](#)]
23. Yeh, D.C.; Huntington, H.B. Extreme Fast-Diffusion System: Nickel in Single-Crystal Tin. *Phys. Rev. Lett.* **1984**, *53*, 1469–1472. [[CrossRef](#)]
24. Feng, J.; Hang, C.; Tian, Y.; Wang, C.; Liu, B. Effect of electric current on grain orientation and mechanical properties of Cu-Sn intermetallic compounds joints. *J. Alloys Compd.* **2018**, *753*, 203–211. [[CrossRef](#)]
25. Oliver, W.C.; Pharr, G.M. An improved technique for determining hardness and elastic modulus using load and displacement sensing indentation experiments. *J. Mater. Res.* **1992**, *7*, 1564–1583. [[CrossRef](#)]
26. Deng, X.; Chawla, N.; Chawla, K.K.; Koopman, M. Deformation behavior of (Cu, Ag)–Sn intermetallics by nanoindentation. *Acta Mater.* **2004**, *52*, 4291–4303. [[CrossRef](#)]